Pores with Longitudinal Irregularities Distinguish Objects by Shape

Yinghua Qiu,[¶,†,‡] Preston Hinkle,[¶,†] Crystal Yang,[¶,§] Henriette E. Bakker,[‖] Matthew Schiel,[†] Hong Wang,[⊥] Dmitriy Melnikov,[#] Maria Gracheva,[#] Maria Eugenia Toimil-Molares,[▽] Arnout Imhof,[‖] and Zuzanna S. Siwy*,[†,§,⊗]

[†]Department of Physics and Astronomy, University of California, Irvine, California 92697, United States, [‡]School of Mechanical Engineering and Jiangsu Key Laboratory for Design and Manufacture of Micro-Nano Biomedical Instruments, Southeast University, Nanjing 211189, China, [§]Department of Chemistry, University of California, Irvine, California 92697, United States, [‖]Soft Condensed Matter, Debye Institute for NanoMaterials Science, Utrecht University, Princetonplein 1, 3584 CC Utrecht, The Netherlands, [⊥]Department of Physics, Nankai University, Tianjin 300457, China, [#]Department of Physics, Clarkson University, Potsdam New York 13699, United States, [▽]Department of Materials Science, GSI Helmholtz Center for Heavy Ion Research, Darmstadt 64291, Germany, and [⊗]Department of Biomedical Engineering, University of California, Irvine, California 92697, United States. [¶]These authors contributed equally.

ABSTRACT The resistive-pulse technique has been used to detect and size objects which pass through a single pore. The amplitude of the ion current change observed when a particle is in the pore is correlated with the particle volume. Up to date, however, the resistive-pulse approach has not been able to distinguish between objects of similar volume but different shapes. In this manuscript, we propose using pores with longitudinal irregularities as a sensitive tool capable of distinguishing spherical and rod-shaped particles with different lengths. The ion current modulations within resulting resistive pulses carry information on the length of passing objects. The performed experiments also indicate the rods rotate while translocating, and displace an effective volume that is larger than their geometrical volume, and which also depends on the pore diameter.
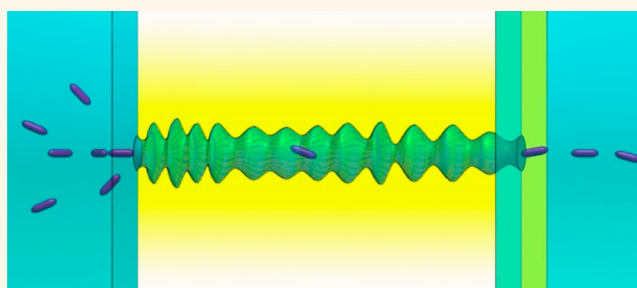
KEYWORDS: resistive-pulse · pore · rod · rotation · excluded volume · electroosmosis

The resistive-pulse technique has been widely applied to size single molecules, viruses, particles and cells.[1−12] A single object passing through a pore causes a transient change of the system resistance, which is detected as a transient change of the transmembrane current, called a resistive-pulse.[6,7] The pulse amplitude is a measure of the object size. while the pulse duration can be correlated with its surface charge.[13−15] Our group has recently hypothesized that transport through pores with undulating diameter can give insight into objects' ability to deform and to quantify their mechanical properties.[16,17] The dynamic size of the transported object was observed by comparing resistive pulses of deformable and hard particles. Undulating pores have therefore potential to provide multipronged physical characterization of passing objects on a single particle level.

In this manuscript we discuss applicability of pores with longitudinal irregularities to extend the resistive-pulse technique even

further to distinguish shapes. Transport of nonspherical particles through pores was discussed in the literature before; however, no solutions were offered as to the pore requirements which would be able to distinguish the shape on a single particle basis.[18] Passage of red-blood cells, whose shape can be approximated as an oblate ellipsoid, produced resistive pulses with oscillating amplitude interpreted as rotations of the cells. A mathematical model was presented which predicted that blockage of the current by a red blood cell depended on the cell orientation with respect to the pore axis.[18] Observation of pulse oscillating amplitude for aspherical objects is possible only for larger objects and in cases where the rotational motion is slower compared to the translocation time. As a result, transport of small aspherical particles would be indistinguishable from the passage of spheres of similar volume. Recently, studies with another type of aspherical particles—rods—have been reported
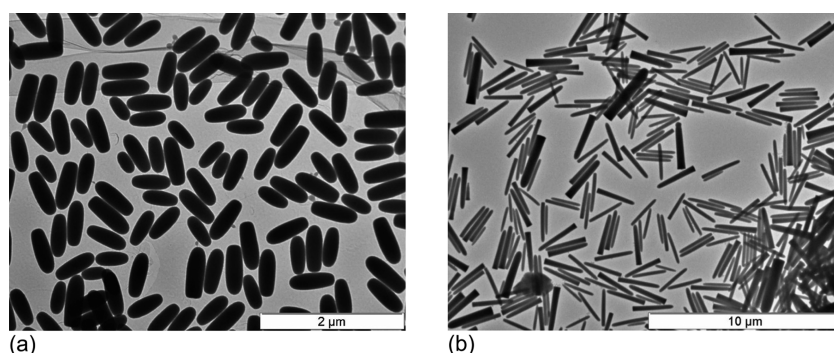
Figure 1. Transmission electron microscope images of the (a) short (230 nm × 590 nm) and (b) long (210 nm × 1950 nm) silica rods used in the reported experiments.

and focused on the ability to probe local structure of the rods,[15,19] or rods aggregation.[20]

Here we present transport of rod shaped particles through ~11 μm long polymer pores whose diameter undulates along the pore axis. Single pores in polyethylene terephthalate (PET) prepared by the track-etching technique were used in the experiments.[21] As shown by our group before, the pores are characterized by significant longitudinal irregularities revealed through resistive-pulse experiments with polystyrene beads as well as metal replicas of the pores.[16,22−24] The diameter undulations of PET pores are attributed to the laminar structure of the films, and penetration of the etchant between the strata.[25] Two types of silica rods[26] with diameters of ~220 nm and lengths of 590 and 1950 nm, respectively, were detected as they electrokinetically passed through single pores with an average opening diameter of ~1 μm. As a comparison, transport of the particles through smooth, cylindrical pores in polycarbonate (PC) was recorded as well. Our results show the shape of resistive pulses in undulating pores can indeed be used as a distinguishing factor between spherical and rod shaped particles. In addition, the recorded pulses of rods suggest that the rods perform rotational motion while translocating, which influences the effective volume they displace, and thus the pulse amplitude. The revolution occurs around the pore axis, and as we expect has a pitch- and yaw-like character leading to an excluded volume equivalent to a double-cone.

RESULTS AND DISCUSSION

Resistive-pulse experiments were first performed with single track-etched polyethylene terephthalate (PET) pores, polystyrene beads, and two types of silica rods (Figure 1).[16,22,23] Figure 2 presents recordings performed with a pore that had an average opening diameter of 770 nm. Each type of particle was studied individually from a suspension in 0.1 M KCl, pH 8 in the presence of Tween 80. The particle suspensions were placed on the same side of the membrane thus all pulses represent passage in the same direction, shown schematically from left to right. Polystyrene particles
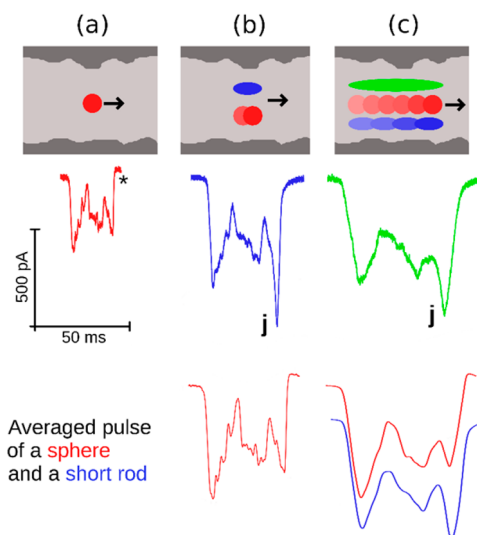

Figure 2. Ion current pulses data and simulated (averaged) traces for three types of particles. Current−time data are shown for (a) a 410 nm diameter sphere (red trace), (b) a 230 nm × 590 nm rod (blue trace), and (c) a 210 nm × 1950 nm rod (green trace). The red trace in (a) was averaged over 11 points to give the simulated red trace in (b), and over 95 points to give the simulated red trace in (c). Similarly, the blue trace in (b) was averaged over 148 points to give the simulated blue trace in (c). The averaged pulses were scaled to facilitate comparison with the raw experimental pulses. Diagrams at the top illustrate particles in the pore for both the data and simulated traces with the same color scheme. Note the distinct current decrease at the exit of the rods, indicated by (j) (see Supporting Information Figure S3), and a current increase at the sphere exit, marked as (*). The pore had an average opening diameter of 770 nm and a length of 11 μm. Current traces were collected at 20 kHz using 0.6 V in 0.1 M KCl at pH 8.

were carboxylated with surface charge of −0.4 e/nm^2 and they moved toward the positively biased electrode. Translocation of silica rods occurred toward the negatively biased electrode, *i.e.*, in the direction of electroosmosis, which is induced by the negative surface charges of the polymer pore walls.[17] Electroosmosis dominated transport of the rods is in agreement with their lower charge density of −0.1 e/nm^2 (ref 27) compared to the spheres (Supporting Information Table S1).

As discussed by us before, ion current pulses corresponding to single spherical particles reflect the pore

topography. *i.e.*, undulations of the diameter along the pore axis.[16,22,23] Passage of the beads through narrower regions causes a larger drop of the current compared to the cases when the same particle passes through wider zones of the pore. These current variations within a pulse were found to be qualitatively independent of the beads diameter in the range between ~200 and ~400 nm.[22] When comparing the shape of pulses in Figure 2, one can notice that some of the pore's finer features are resolved by spheres but not by the rods. The rods' signals seem "smoothed out" (Figure 2b,c, blue and green signals), while the averaged pulses of a spherical particle are indeed very similar to pulses created by the rods (Figure 2b,c, red).

When choosing the number of points to average over, we first calculated the time it would take a sphere to travel a distance such that the sphere sweeps out the length of a rod. By multiplying this time by the sampling rate of our data acquisition, we obtained the number of data points to average over to accurately simulate the rod's signal. For example, the 410 nm sphere travels a distance (L_{rod} − 410 nm) equal to 180 nm in sweeping out the full length of the shorter type of rod (scheme in Figure 2b). We assume the velocity of the sphere, $v_{translocation}$, is constant while in the pore, and therefore its magnitude is equal to the length of the pore (11 μm) divided by the translocation time (34 ms): this yields $v_{translocation}$ = 0.32 μm/ms. Therefore, the time it takes the sphere to sweep out the shorter rod's length is 0.56 ms, which when multiplied by the sampling rate of 20 kHz yields the number of points to average over, which is in this case 11. This smoothing process also provided indirect evidence for the translocation of individual rods and that the two types of rods differ in length. A comparative analysis of pulses of spheres with known diameter and pulses of unknown rods can therefore yield information on the rod length.

The averaging process for the spheres however could not capture the distinct current decrease at the rods' exit (marked as (j) in Figure 2), especially pronounced in the events caused by the longer rods (Figure 2c). To understand the origin of the pulse shape for rods, we translocated the same rod in both directions by reversing the voltage polarity. The large current decrease at the pulse end was present in pulses of the particles passing in both directions, indicating this feature of resistive pulses is related to the particle exit and not to how the rods probe the pore topography (Supporting Information Figure S1).

On the basis of previous studies with spherical and charged particles, we hypothesized that the rods change the expected current values at the pulse end by modulating local ionic concentrations near pore entrances.[23,28] Negatively charged particles, when present at the pore entrance on the same side as the negatively biased electrode, were found to decrease concentration of anions observed as a current decrease. Since rods pass in the direction of electroosmosis, *i.e.*, toward the negatively biased electrode, the enhanced current decrease is present at the end of the translocation. To provide evidence for the role of the particle surface charges in the formation of this feature of resistive pulses for rods, experiments of rods passage were also performed in 0.3 M KCl. The higher ionic strength was expected to provide better screening of the charges, so that their influence on ionic current when the particle is at the pore exit would be smaller. In line with our predictions, the relative current decrease at the pulse end at the higher concentration was less pronounced compared to the recordings in 0.1 M KCl (Supporting Information Figure S2). The current decrease is expected to last longer and be more dominant for rods due to their elongated shape, so that the part of the rod which is already outside the pore influences the access of ions and ion current while the remaining part is exiting. Note that the exit effect of the spheres is much less pronounced and visible only as a small current increase of the current above the baseline at the end of the pulse (marked as an asterisk (*) in Figure 2). As discussed by us before, a charged sphere at the pore entrance in contact with a positively biased electrode indeed enhances cationic concentration and measured current.[23] Since the exit effects are related with the charge of translocating particles, their direction of transport, and potentially even chemical properties, they carry only limited information on the particle shape, and as shown below should not be taken into account in a quantitative analysis.

The frequency of rods passage in 0.3 M KCl was a few times lower compared to the event frequency in 0.1 M KCl, which we think is related with the tendency of rods to aggregate at the higher ionic strength. A similar observation was made before in resistive pulse experiments with hydrogels.[16,29] The remaining experiments were therefore performed in 0.1 M KCl.

As the next step we analyzed the pulses quantitatively and checked whether the pulse amplitude could be correlated with the object volume (Figure 3). Average current blockage, ΔI, caused by each particle was calculated by integration of its pulse, and expressed as a relative current change $\Delta I/I_p$, where I_p stands for ion current with the particle; I_p was calculated as a difference between the baseline current and ΔI. Due to the large current decrease at the end of rod events, the magnitude of ΔI was calculated based only on the part of the pulse whose features could be correlated with the pulses of spheres through the same pore (between peaks a and g shown in Supporting Information Figure S3).

The relative depth of a resistive pulse for a spherical particle can be predicted from the following equation:[6,9,22]

$$\frac{R_p - R_e}{R_e} = \frac{I_e - I_p}{I_p} = \frac{d^3}{D^2L}S\left(\frac{d}{D}\right) \quad (1)$$
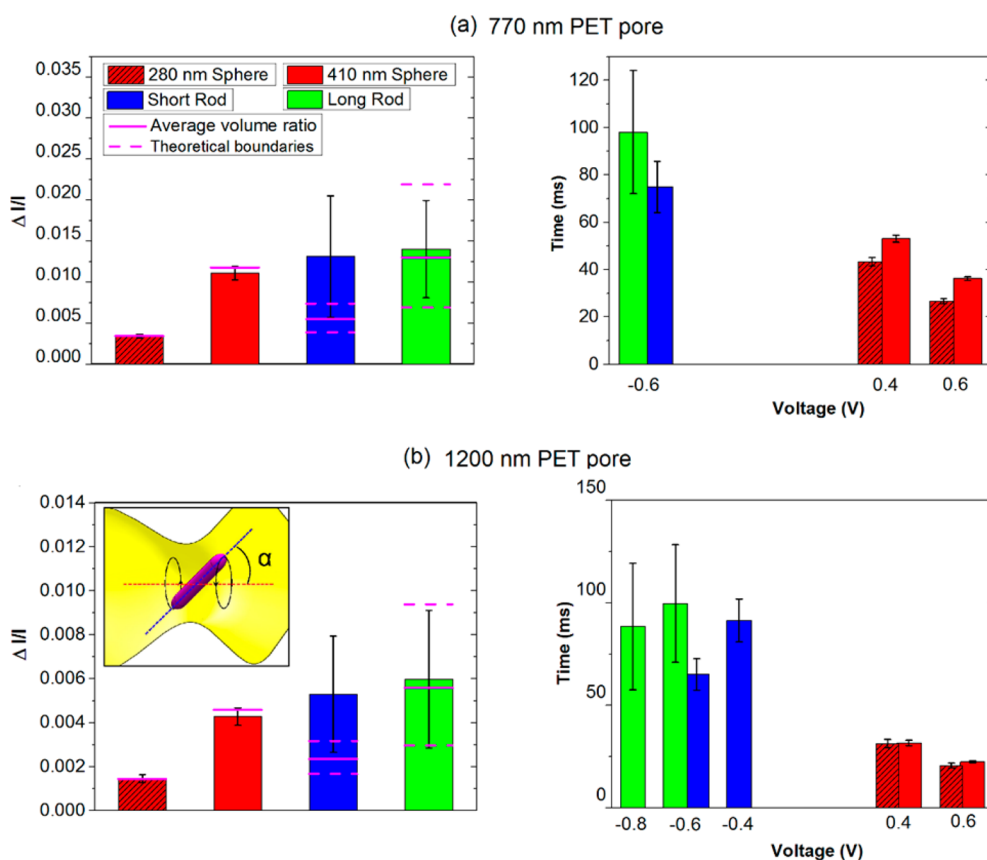
Figure 3. Analysis of resistive pulses obtained with spherical polystyrene particles and two types of silica rods through two PET pores with an average opening diameter of 770 nm (a) and 1200 nm (b). Left panels show the dependence of the pulse amplitude on the type of particle. Magenta solid lines indicate predicted current change based on eqs 1 and 3 for $\alpha = 0$; magenta dashed lines indicate the predicted $\Delta I/I$ for rods whose length and width are one standard deviation above and below the average values. Right panels show voltage dependence of the translocation times. An inset in (b) schematically shows rods' revolution around the pore axis. All recordings were performed in 0.1 M KCl, pH 8. In each experiment at least 200 events of individual particles were recorded, one standard deviation of which is indicated by the error bars. Note that $\Delta I/I$ for 280 nm particles was used as a basis for calculating the average pore opening diameter.

where d and D are the particle and pore diameters, respectively, and L is the pore length. R_p and R_e (I_p and I_e) indicate the electrical resistance (ion current) with and without a particle in a pore. The proportionality coefficient, $S(d/D)$, is the so-called shape factor and has the following form:

$$S\left(\frac{d}{D}\right) = \left[1 - 0.8\left(\frac{d}{D}\right)^3\right]^{-1} \qquad (2)$$

which for the 770 nm pore and 410 nm particles predicts the $\Delta I/I$ equal 0.012 and thus, is in a good agreement with the experiments (Figure 3).

The amplitude of resistive pulses of rods can be estimated by approximating their cylindrical shape by a prolate ellipsoid, and using well-tabulated demagnetization and electrical shape factors.[18,30] The magnitude of $\Delta R/R$ can be related with the pore and particle volumes, V and v, respectively, as[18]

$$\frac{\Delta R}{R} = [f_- + (f_{||} - f_-)\cos^2\alpha]v/V \qquad (3)$$

where f_- and $f_{||}$ are electrical shape factors and α is the angle between the field and the axis of revolution. For the shorter rods, $f_- = 1.75$ and $f_{||} = 1.17$; for the longer rods $f_- = 2.0$ and $f_{||} = 1.0$.[18] The predicted pulse amplitude for the shorter rods in the 770 nm pore with $\alpha = 0$ is however significantly lower than the values measured experimentally (Figure 3a); increasing the value of α in eq 3 did not significantly improve the fitting until 90°, which would be difficult to achieve due to steric hindrance in the submicrometer pore. It is important to note that the recorded pulses of the shorter rods had larger amplitude than the pulses of the spheres even though the volume of these 410 nm beads is larger than the volume of the 230 × 590 nm rods. Equation 3, however, correctly described the experimentally observed current blockage for the longer rods (Figure 3a). Similar conclusions were drawn based on data recorded with a different membrane containing a pore with an average diameter of 1200 nm (Figure 3b).

To explain the large pulse amplitude of the shorter rods, we consider a possibility the particles perform

rotational motion, *i.e.*, revolution around the pore axis, and hypothesize that the effective volume a rod displaces is equal to the volume of two cones (inset to Figure 3). Although the rods were shown before to orient with the direction of externally applied electric field,[26,31] due to the undulating diameter of PET pores, different parts of the rods will be subjected to different local electric fields, making their axial alignment unstable. The resulting torque, T_e, will induce a pitch- and yaw-like motion of the rods (Figure 3), and will be balanced by the frictional torque resisting this motion:

$$T_e = f_r \omega \qquad (4)$$

where ω is rotational speed in rad/s, and f_r is the frictional coefficient for rotation, which can be calculated from the Einstein−Smoluchowski equation. First we found the rods' rotational diffusion coefficient, D_{diff}, based on the analysis and equations derived in ref 32. The estimated diffusion coefficient in the bulk for the two considered rods is 13 and 0.8 rad/s. The frictional coefficient, f_r, can be then calculated as $k_B T/D_{diff}$, where k_B is the Boltzmann constant and T is temperature.

To quantify the electric torque acting on a rod, T_e, we considered a 10 μm long model pore containing undulations such that the diameter was changing between 1000 and 1100 nm. The length of each undulation was assumed 2000 nm. The electric force acting on rod's ends present in two zones with different opening diameter will differ by a factor of 1.2, and depending on the rod position along the pore axis, it will cause clockwise or anticlockwise motion. The torque can then be calculated knowing the difference of the forces acting on rod ends (found from electric field and surface charge) and the distance from the center of rotation. The maximum torque occurs when the rod is halfway between two regions. In this case, each half of the rod has total charge equal to the half of the total charge of the rod, calculated assuming the surface charge density of −0.1 e/nm². When 1 V is applied across the membrane, ω is estimated to be 10^4 rad/s. Rotations of the rods are therefore much faster than the rod translocations (Figure 3), even if one considers a possible reduction of diffusion coefficient in the pore.[33,34] The calculations support our hypothesis that on the time scale of the transport, the rods might indeed be equivalent to a larger volume of two cones, the shape which a rod could sweep out during its revolution around the pore axis (inset to Figure 3b). The rods' revolution might in addition be masked and averaged by the pore undulating diameter. To resolve individual revolutions, the sampling frequency would have to be increased so that submicrosecond processes could be observed. We plan to do it by redesigning the experimental setup to reduce the system capacitance, which is needed to improve signal-to-noise ratio at higher frequencies. Reducing capacitance will be achieved by using thicker membranes

and limiting the membrane area exposed to the electrolyte solution.

In the analysis we focused on the role of electric torque in inducing rods' revolution around the pore axis. It is also possible that due to the electroosmotic flow of the whole solution, the shear stress present in the fluid flow contributes to the rods' rotation as well.[18]

The hypothesis on rotation of the shorter rods is also corroborated by the experimental observation of a smaller effective volume the rods displace in a narrower pore in which the revolution around the pore axis is expected to be hindered by the proximity to the walls (compare the calculated displayed volume for 1550 and 770 nm pores, Supporting Information Figure S4). Revolution of the longer rods is most probably negligible since their length is significantly larger than the pore diameter. The predicted rotational speed of the longer rods based on eq 4 is a few times lower than the magnitude of ω for the shorter rods.

To understand the role of diameter undulations on the ability to distinguish rods from spheres, control resistive pulse experiments were performed with single track-etched polycarbonate pores. Due to the amorphous structure of this polymer, pores created in this material are smooth and nearly ideally cylindrical.[24] This experiment was also important in understanding the role of pore undulations in the rods' rotation and effective excluded volume. Figure 4 shows example resistive pulses obtained with polystyrene 410 nm spheres and the short silica rods. The pulses have primarily a rectangular shape confirming the pore is indeed cylindrical. The large current decreases in the beginning and at the end of the pulses as well as metal replica of the pores (Supporting Information Figure S5) suggest both entrances are narrower than the middle part of the pore. A similar pulse has been obtained with PMMA particles (not shown) indicating the current spikes are indeed due to the pore geometry and not modulations of ionic concentrations by charged particles.[23] Passage of 410 nm spheres confirmed that the pore in the middle is ~930 nm in diameter, and the values of $\Delta I/I$ have been calculated based on the current in the flat, middle region. Figure 4 also shows experimentally measured and predicted from eqs 1 and 3 magnitudes of current blockage caused by the spheres and 590 nm long rods. The experiments indicate that a volume excluded by the rods is again larger than predicted based on the rod's geometrical volume, suggesting the rods are performing rotation. We hypothesize that rods' revolution along the axis of smooth polycarbonate pores can occur due to the shear stress present in the fluid flow.[18] Comparing the magnitude of measured and predicted $\Delta I/I$, we noticed that the discrepancy for the rods in the polycarbonate pore is smaller compared to values obtained in PET pores (Figures 3 and 4), suggesting
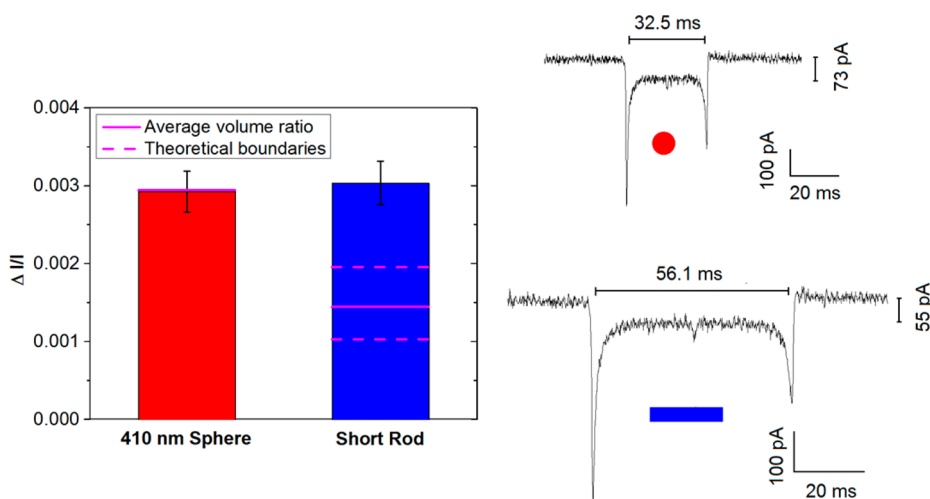
Figure 4. Resistive pulse experiments in a 930 nm in diameter polycarbonate pore performed with 410 nm spherical particles and 230 nm × 590 nm silica rods. Average amplitude of the pulses and example pulse shapes are shown. These experiments were performed in 0.1 M KCl, pH 10 to enhance surface charge on polycarbonate pores. The spherical particles passed toward the positively biased electrode (0.6 V), while the rods translocated for the opposite voltage polarity (−1 V). The relative current change is voltage independent.

the rotational freedom can be reduced by smooth pores. Indeed, the amplitudes of pulses of the 410 nm beads and the shorter rods are comparable; in all studied PET pores, the rod amplitude was the highest. Resistive pulses of spheres and rods obtained in the polycarbonate pore (Figure 4) clearly indicate that only pores with multiple undulations facilitate distinguishing shapes of the passing objects.

Our original motivation for the experiments was to explore the possibility of using the resistive-pulse technique to characterize particles by their shape. Recordings in Figure 2 indicate that spherical and cylindrical shapes can be distinguished from each other in rough pores based on the characteristics of ion current pulses they cause. Namely, spherical particles resolve the pore internal topography with higher resolution than elongated particles. Indeed, averaging the ion current signal of spheres results in pulses which resemble the recordings created by the rods (Figure 2). In addition, the excluded volume of aspherical particles with length smaller than the average pore diameter depends on the pore diameter, being lower in narrower pores and in smooth pores. Thus, a protocol which could be used to characterize an unknown solution of particles would involve passage of a set of spheres and the unknown particles through at least two rough pores with different average opening diameters, and through a smooth pore. An elongated character and length of tested particles would be established by comparing their pulses with these created by spheres. Presence of rotations could be tested by checking for the dependence of the excluded volume on pore diameter and pore smoothness.

When performing analysis of unknown particles it will also be important to probe both voltage polarities so that electroosmosis or electrophoresis dominated

transport can be observed. The applied voltage will have to be sufficiently high to allow one to resolve ion current undulations within a resistive pulse. In our experiments with ~1 μm in diameter pores, particle translocations could be observed and resolved for voltages below 1 V (Supporting Information Figure S6). Choice of bulk electrolyte concentration should be dictated by the signal-to-noise ratio, which increases with the increase of salt concentration,[23] and considerations of the possible aggregation of the studied particles. We expect that 100 mM will be optimal for detection and characterization of many types of particles, assuring high signals and preventing particle aggregation. As shown by us before, resistive-pulses for a given pore recorded in various concentrations preserve the main features of ion current undulations, except the exit effects, which become more pronounced at low concentrations.[23]

CONCLUSIONS

The manuscript presents experimental studies of passage of spherical particles and rods through large aspect ratio pores characterized with longitudinal irregularities. The shape of current pulses depends on the shape and length of the particles giving the basis for a facile distinction between objects of different shapes. Axially varying pore diameter was found to be crucial in the ability to distinguish the objects by shape; pulses created by spheres and rods in a smooth pore were indistinguishable from each other.

The experiments also indicate that in pores whose diameter is comparable or larger than the rod length, the passing rods exhibit revolution around the pore axis. As a result, the volume excluded by the rotating rods is larger than their geometrical volume, and depends on the pore opening diameter. We have

suggested a protocol of examining an unknown suspension of particles, which involves comparative studies with spherical particles and using pores with different average opening diameter. In our future studies, we will focus on redesigning the experimental setup in order to reduce the system capacitance and to access rods' individual revolutions at the submicrosecond time scale.

Modulations of ion current signal by rods' rotation are expected to provide additional information on the object volume.

We expect that the ability to determine shape of meso and nano-objects will be important for many applications, including examination of particles used, *e.g.*, in medicine, and in virus characterization.[10−12,19,35−37]

EXPERIMENTAL METHODS

Preparation of Pores. Single pores in 12 μm thick films of polyethylene terephthalate (PET) were prepared by the track-etching technique as described before.[16,22,23] Briefly, the films were irradiated with single energetic heavy ions (*e.g.*, 11.4 MeV/u Au and U ions) at the UNILAC linear accelerator of the GSI Helmholtzzentrum für Schwerionenforschung in Darmstadt, Germany. Wet chemical etching of the films in 0.5 M NaOH, 70 °C leads to preparation of pores with undulating pore diameter along the pore axis. The mean pore diameter was estimated from the current−voltage measurements performed in 1 M KCl, and relating the pore diameter with its conductance.[38,39] The opening diameter was subsequently confirmed using resistive-pulse technique with 280 nm in diameter particles. Opening diameters determined by the two approaches, electrochemical and resistive-pulse, did not differ from each other by more than 15%. Presented here are experiments that were performed with pores with an average opening diameter between 770 and 1550 nm. The walls of track-etched PET pores contain carboxyl groups and are negatively charged at pH values above 3.8.[38]

Control experiments were performed with track-etch pores created in 30 μm thick polycarbonate (PC) films. Etching of single-ion irradiated PC films was done in 5 M NaOH, 50 °C, which, as shown before,[24] leads to preparation of smooth, cylindrically shaped nanopores. Similar to pores in PET, track-etched PC pores are characterized with negative surface charge at pH values above 4.

Particles. Polystyrene particles with diameter of 280 and 410 nm were purchased from Bangs Laboratory, Inc. Silica rods were synthesized as described before.[26] Briefly, 30 g of poly-(vinylpyrrolidone) (PVP, M_w = 40 000, Sigma-Aldrich) was dissolved in 300 mL of 1-pentanol ($\geq$99%, Sigma-Aldrich) by sonication. After PVP had dissolved, 30 mL of absolute ethanol (Baker), 8.4 mL of ultrapure water (Millipore system), and 2 mL of 0.18 M sodium citrate dibasic sesquihydrate (99%, Sigma-Aldrich) were added and the flask was shaken. Then, 6.75 mL of ammonia (25%, Merck) was added and the flask was shaken again. Finally, 2.5 mL of tetraethyl orthosilicate (TEOS, $\geq$ 98%, Fluka) was added. After the obtained emulsion had been shaken again, the reaction mixture was left to rest overnight. This resulted in silica rods with an average length L = 590 nm (polydispersity σ_L = 15%), diameter D = 230 nm (σ_L = 8%), and aspect ratio L/D = 2.6. Longer rods were made using the same procedure, but with sodium citrate dihydrate instead of sodium citrate dibasic sesquihydrate, and at a smaller volume: 100 mL 1-pentanol, 10 mL absolute ethanol, 2.5 mL water, 1 mL 0.18 M sodium citrate dihydrate, 2 mL ammonia, and 1 mL TEOS. The long rods had L = 1950 nm (σ_L = 14%), D = 210 nm (σ_L = 21%), and aspect ratio of L/D = 9.2. Figure 1 shows transmission electron microscopy (TEM) images of the particles used in the study.

Ion Current Recordings and Particle Detection. Resistive-pulse experiments were performed on suspensions prepared in 100 mM KCl, pH 8 and pH 10, containing 0.1% of Tween 80. A few measurements were also performed using 300 mM KCl. The concentration of the spherical particles was 10^9 particles/mL. Detection of rods was performed with suspensions containing between 10^6 and 10^8 rods/mL. A particle suspension was placed on one side of the membrane, while the other side was in contact with 100 mM (or 300 mM) KCl. Ion current measurements were performed with Axopatch 200B and 1322A Digidata (Molecular Devices, Inc.) using sampling frequency of 20 kHz. The data were subjected to low-pass Bessel filter of 1 kHz. The voltage sign was determined with respect to the side without particles.

REFERENCES AND NOTES

1. Kasianowicz, J. J.; Brandin, E.; Branton, D.; Deamer, D. W. Characterization of Individual Polynucleotide Molecules Using a Membrane Channel. *Proc. Natl. Acad. Sci. U.S.A.* **1996**, *93*, 13770–13773.

2. Venkatesan, B. M.; Bashir, R. Nanopore Sensors for Nucleic Acid Analysis. *Nat. Nanotechnol.* **2011**, *6*, 615–624.

3. Cherf, G. M.; Lieberman, K. R.; Rashid, H.; Lam, C. E.; Karplus, K.; Akeson, M. Automated Forward and Reverse Ratcheting of DNA in a Nanopore at 5-Å Precision. *Nat. Biotechnol.* **2012**, *30*, 344–348.

4. Manrao, E. A.; Derrington, I. M.; Laszlo, A. H.; Langford, K. W.; Hopper, M. K.; Gillgren, N.; Pavlenok, M.; Niederweis, M.; Gundlach, J. H. Reading DNA at Single-Nucleotide Resolution with a Mutant MspA Nanopore and Phi29 DNA Polymerase. *Nat. Biotechnol.* **2012**, *30*, 349–354.

5. Movileanu, L. Squeezing a Single Polypeptide Through a Nanopore. *Soft Matter* **2008**, *4*, 925–931.

6. Coulter, W. H. Means for Counting Particles Suspended in a Fluid. U.S. Pat. No. 2,656,508, 1953.

7. DeBlois, R. W.; Bean, C. P.; Wesley, R. K. A. Electrokinetic Measurements with Submicron Particles and Pores by the Resistive Pulse Technique. *J. Colloid Interface Sci.* **1977**, *61*, 323–335.

8. Berge, L. I.; Feder, J.; Jøssang, T. A Novel Method to Study Single-Particle Dynamics by the Resistive Pulse Technique. *Rev. Sci. Instrum.* **1989**, *60*, 2756–2763.

9. DeBlois, R. W.; Bean, C. P. Counting and Sizing of Submicron Particles by the Resistive Pulse Technique. *Rev. Sci. Instrum.* **1970**, *41*, 909–916.

10. DeBlois, R. W.; Wesley, R. K. A. Sizes and Concentrations of Several Type C Oncornaviruses and Bacteriophage T2 by the Resistive-Pulse Technique. *J. Virol.* **1977**, *23*, 227–233.

11. Harms, Z. D.; Mogensen, K. B.; Nunes, P. S.; Zhou, K.; Hildenbrand, B. W.; Mitra, I.; Tan, Z.; Zlotnick, A.; Kutter, J. P.; Jacobson, S. C. Nanofluidic Devices with Two Pores in Series for Resistive-Pulse Sensing of Single Virus Capsids. *Anal. Chem.* **2011**, *83*, 9573–9578.

12. Zhou, K.; Li, L.; Tan, Z.; Zlotnick, A.; Jacobson, S. C. Characterization of Hepatitis B Virus Capsids by Resistive-Pulse Sensing. *J. Am. Chem. Soc.* **2011**, *133*, 1618–1621.

13. Ito, T.; Sun, L.; Crooks, R. M. Simultaneous Determination of the Size and Surface Charge of Individual Nanoparticles Using a Carbon Nanotube-Based Coulter Counter. *Anal. Chem.* **2003**, *75*, 2399–2406.

14. Kozak, D.; Anderson, W.; Vogel, R.; Chen, S.; Antaw, F.; Trau, M. Simultaneous Size and ζ-Potential Measurements of Individual Nanoparticles in Dispersion Using Size-Tunable Pore Sensors. *ACS Nano* **2012**, *6*, 6990–6997.

15. Venta, K. E.; Zanjani, M. B.; Ye, X.; Danda, G.; Murray, C. B.; Lukes, J. R.; Drndic, M. Gold Nanorod Translocations and Charge Measurements through Solid-State Nanopores. *Nano Lett.* **2014**, *14*, 5358–5364.

16. Pevarnik, M.; Schiel, M.; Yoshimatsu, K.; Vlassiouk, I.; Kwon, J. S.; Shea, K. J.; Siwy, Z. S. Particle Deformation and Concentration Polarization in Electroosmotic Transport of Hydrogels through Pores. *ACS Nano* **2013**, *7*, 3720–3728.

17. Innes, L.; Chen, C.-H.; Schiel, M.; Pevarnik, M.; Haurais, F.; Tomil-Molares, E.; Vlassiouk, I. V.; Theogarajan, L.; Siwy, Z. S. Velocity Profiles in Pores with Undulating Opening Diameter and Their Importance for Resistive-Pulse Experiments. *Anal. Chem.* **2014**, *86*, 10445–10453.

18. Golibersuch, D. C. Observation of Aspherical Particle Rotation in Poiseuille Flow *via* the Resistance Pulse Technique. *Biophys. J.* **1973**, *13*, 265–280.

19. McMullen, A.; de Haan, H. W.; Tang, J. X.; Stein, D. Stiff Filamentous Virus Translocations through Solid-State Nanopores. *Nat. Commun.* **2014**, *5* (4171), 1–10.

20. Platt, M.; Willmott, G. R.; Lee, G. U. Resistive Pulse Sensing of Analyte-Induced Multicomponent Rod Aggregation Using Tunable Pores. *Small* **2012**, *8*, 2436–2444.

21. Fleischer, R. L.; Price, P. B.; Walker, R. M. *Nuclear Tracks in Solids: Principles and Applications*; University of California Press: Berkeley CA, 1975.

22. Pevarnik, M.; Healy, K.; Toimil-Molares, M. E.; Morrison, A.; Létant, S. E.; Siwy, Z. S. Polystyrene Particles Reveal Pore Substructure as They Translocate. *ACS Nano* **2012**, *6*, 7295–7302.

23. Menestrina, J.; Yang, C.; Schiel, M.; Vlassiouk, I.; Siwy, Z. S. Charged Particles Modulate Local Ionic Concentrations and Cause Formation of Positive Peaks in Resistive-Pulse-Based Detection. *J. Phys. Chem. C* **2014**, *118*, 2391–2398.

24. Müller, S.; Schötz, C.; Picht, O.; Sigle, W.; Kopold, P.; Rauber, M.; Alber, I.; Neumann, R.; Toimil-Molares, M. E. Electrochemical Synthesis of $Bi_{1-x}Sb_x$ Nanowires with Simultaneous Control on Size, Composition, and Surface Roughness. *Cryst. Growth Des.* **2012**, *12*, 615–621.

25. Mukaibo, H.; Horne, L. P.; Park, D.; Martin, C. R. Controlling the Length of Conical Pores Etched in Ion-Tracked Poly-(ethylene terephthalate) Membranes. *Small* **2009**, *5*, 2474–2479.

26. Kuijk, A.; van Blaaderen, A.; Imhof, A. Synthesis of Monodisperse, Rodlike Silica Colloids with Tunable Aspect Ratio. *J. Am. Chem. Soc.* **2011**, *133*, 2346–2349.

27. Sonnefeld, J.; Göbel, A.; Vogelsberger, W. Surface Charge Density on Spherical Silica Particles in Aqueous Alkali Chloride Solutions. *Colloid Polym. Sci.* **1995**, *273*, 926–931.

28. Lan, W.-J.; Kubeil, C.; Xiong, J.-W.; Bund, A.; White, H. S. Effect of Surface Charge on the Resistive Pulse Waveshape During Particle Translocation through Glass Nanopores. *J. Phys. Chem. C* **2014**, *118*, 2726–2734.

29. Holden, D. A.; Hendrickson, G.; Lyon, L. A.; White, H. S. Resistive Pulse Analysis of Microgel Deformation During Nanopore Translocation. *J. Phys. Chem. C* **2011**, *115*, 2999–3004.

30. Osborn, J. A. Demagnetizing Factors of the General Ellipsoid. *Phys. Rev.* **1945**, *67*, 351–357.

31. Liu, B.; Besseling, T. H.; Hermes, M.; Demirörs, A. F.; Imhof, A.; van Blaaderen, A. Switching Plastic Crystals of Colloidal Rods with Electric Fields. *Nat. Commun.* **2014**, *5* (3092), 1–8.

32. Tirado, M. M.; de la Torre, J. G. Rotational Dynamics of Rigid, Symmetric Top Macromolecules. Application to Circular Cylinders. *J. Chem. Phys.* **1980**, *73*, 1986–1993.

33. Pagliara, S.; Schwall, C.; Keyser, U. F. Optimizing Diffusive Transport through a Synthetic Membrane Channel. *Adv. Mater.* **2013**, *25*, 844–849.

34. Schiel, M.; Siwy, Z. S. Diffusion and Trapping of Single Particles in Pores with Combined Pressure and Dynamic Voltage. *J. Phys. Chem. C* **2014**, *118*, 19214–19223.

35. Longmire, M.; Choyke, P. L.; Kobayashi, H. Clearance Properties of Nano-Sized Particles and Molecules as Imaging Agents: Considerations and Caveats. *Nanomedicine* **2008**, *3*, 703–717.

36. Champion, J. A.; Katare, Y. K.; Mitragotri, S. Particle Shape: A New Design Parameter for Micro- and Nanoscale Drug Delivery Carriers. *J. Controlled Release* **2007**, *121*, 3–9.

37. Mitragotri, S.; Lahann, J. Physical Approaches to Biomaterial Design. *Nat. Mater.* **2009**, *8*, 15–23.

38. Ermakova, L. E.; Sidorova, M. P.; Bezrukova, M. E. Filtration and Electrokinetic Characteristics of Track Membranes. *Colloid J.* **1998**, *52*, 705–712.

39. Apel, P.; Korchev, Y. E.; Siwy, Z.; Spohr, R.; Yoshida, M. Diode-Like Single-Ion Track Membrane Prepared by Electro-Stopping. *Nucl. Instrum. Methods Phys. Res., Sect. B* **2001**, *184*, 337–346.